R e s e a r c h   a r t i c l e

urn:lsid:zoobank.org:pub:C36434E5-E7E4-4BD8-A34C-8316380635C5

A new species and a new record of Cirratulidae (Annelida, Cirratulida) from Loki's Castle vent field

Maël GROSSE [1,*], Jon Anders KONGSRUD [2], Tom ALVESTAD [3],
Mari Heggernes EILERTSEN [4] & Nataliya BUDAEVA [5]

[1] Natural History Museum, University of Oslo, 0562 Oslo, Norway.
[1] Department of Biology, University of the Balearic Islands, 07122 Palma, Spain.
[2,3,5] Department of Natural History, University Museum of Bergen, University of Bergen,
Postboks 7800, 5020 Bergen, Norway.
[4] Department of Biological Sciences, University of Bergen, Postboks 7800, 5020 Bergen, Norway.
[4] Centre for Deep Sea Research, University of Bergen, Postboks 7803, 5020 Bergen, Norway.

[1] Corresponding author: maelgrosse@gmail.com
[2] Email: Jon.Kongsrud@uib.no
[3] Email: Tom.Alvestad@uib.no
[4] Email: Mari.Eilertsen@uib.no
[5] Email: Nataliya.Budaeva@uib.no

[1] urn:lsid:zoobank.org:author:A14165B0-F030-43AD-887D-3A34C8BA8CB3
[2] urn:lsid:zoobank.org:author:4AF3F49E-9406-4387-B282-73FA5982029E
[3] urn:lsid:zoobank.org:author:8A7B0958-8630-42E5-B957-B9DCD308D031
[4] urn:lsid:zoobank.org:author:9A3374C8-30FF-435C-AF67-100E33E14EAE
[5] urn:lsid:zoobank.org:author:F6894CCF-E8F7-489A-88F3-834D1684E7DE

Abstract. Deep-sea research is a very active field in which environments such as hydrothermal vents are of particular interest because they host a unique and often endemic fauna. In this paper, we describe a new species of the genus *Caulleriella* Chamberlin, 1919 (Annelida, Cirratulidae Ryckholt, 1851) and report the presence of *Raricirrus arcticus* Buzhinskaja & Smirnov, 2017 at Loki's Castle vent field (LCVF), which is the first detailed report of this species since the original description. Both species are illustrated and similarities with closely related species are discussed. We provide genetic data for COI, 16S and 28S for both species. Phylogenetic analyses confirm the identity of each species and the monophyly of each genus. *Caulleriella jormungandri* sp. nov., in addition to being common at LCVF, is recorded from stations without any known chemosynthesis-based environments, suggesting this species to be a part of the background fauna. *Raricirrus arcticus* was originally described from a cold seep, and with the new records from the Loki's Castle hydrothermal vent, it is considered to be a specialist of chemosynthesis-based ecosystems and the geographic distribution of the species is vastly expanded from the Laptev Sea to the Nordic Seas.

Keywords. Deep-sea, North-East Atlantic, *Caulleriella*, *Raricirrus*, polychaetes.

Introduction

Hydrothermal vents are present along all oceanic ridges as well as in back-arc basins and at some seamounts (Van Dover *et al*. 2002). They are punctual areas of the seafloor from which hot and mineral-rich water springs out, creating unique environments known to host highly specialised biological communities (Ramirez-Llodra *et al*. 2007). Loki's Castle vent field (LCVF) is a black smoker vent field that was discovered on the Arctic Mid-Ocean Ridge (AMOR) in 2008 (Pedersen *et al*. 2010). LCVF hosts a unique biodiversity of specialised and opportunistic species (Eilertsen *et al*. 2024), and several species have been described from this locality including annelids of the families Ampharetidae Malmgren, 1866, Maldanidae Malmgren 1867, and Orbiniidae Hartman, 1942 (Kongsrud & Rapp 2012; Kongsrud *et al*. 2017; Meca *et al*. 2024). The highest species richness in the LCFV is found in the diffuse-venting areas which host a biogenic habitat dominated by the siboglinid *Sclerolinum contortum* Smirnov, 2000 together with other annelids that contribute to the structure of the 'worm forests', such as *Oligobrachia* sp. and *Nicomache lokii* Kongsrud & Rapp, 2012 (Kongsrud & Rapp 2012; Eilertsen *et al*. 2024). Two species of Cirratulidae Ryckholt, 1851 were reported from this site in a recent checklist of the field's fauna: *Raricirrus arcticus* Buzhinskaja & Smirnov, 2017 and a putatively new species of *Caulleriella* Chamberlin, 1919 (Eilertsen *et al*. 2024). However, no detail or specific description was given in this publication.

Until now, three species of Cirratulidae have been reported from hydrothermal vent areas: *Raricirrus arcticus*, *Raricirrus jennae* Magalhães Linse & Wiklund, 2017 and *Cirratulus incertus* McIntosh, 1916 (Sweetman *et al*. 2013). However, it is likely that more species have been reported from various vent and seep sites across the globe under identification at the family level (Ritt *et al*. 2010; Sellanes *et al*. 2011; Zapata-Hernández *et al*. 2014) or at the genus level (Kelley & Shank 2010; Schander *et al*. 2010; Sellanes *et al*. 2011; Portail *et al*. 2016; Alalykina 2022). In total, six genera out of 16 in the family Cirratulidae have been recorded at vents and seep sites: *Cirratulus* Lamarck, 1818, *Caulleriella* Chamberlin, 1919, *Raricirrus* Hartman, 1961, *Dodecaceria* Örsted, 1843, *Aphelochaeta* Blake, 1991 and *Chaetozone* Malmgren, 1867.

Caulleriella is a genus in the family Cirratulidae, characterised by the presence of bidentate spines at least in the neuropodia, and a large distance between neuropodia and notopodia (Blake 2021). This genus comprises 49 accepted species widely distributed across the globe from intertidal sediments (e.g., Dean & Blake 2007) to abyssal depths (e.g., Blake 2019). Several species have recently been described from the deep sea (e.g., Blake 2018, 2021). One unidentified species of *Caulleriella* has been reported from the Lost City hydrothermal field on the mid Atlantic ridge (Kelley & Shank 2010). *Raricirrus* is characterised by its small body size, low number of segments, lack of tentacles, the presence of a few dorsal branchiae limited to anterior segment and diverse types of chaetae including serrated capillaries, falcate, pectinate and serrated chaetae and spines (Magalhães *et al*. 2017). This small genus includes seven species, all of which are associated with reducing environments such as organically enriched sediments, woodfalls or whale skeletons (Dean 1995; Buzhinskaja & Smirnov 2017; Magalhães *et al*. 2017; Jimi *et al*. 2022).

In this paper, we describe a new species, *Caulleriella jormungandri* sp. nov., and provide additional information to the description of *Raricirrus arcticus* from LCVF. Both species are studied and illustrated using light and scanning electron microscopy (SEM). Sequences of COI, 16S and 28S are provided to assess phylogenetic position of the species within Cirratulidae.

Material and methods

Study area and cruises

Specimens from LCVF were collected during seven cruises with R/V *G.O. Sars* between 2008 and 2019 organised by the Centre for Geobiology (2008–2017) and KG Jebsen Centre for Deep Sea Research (2017–2019) using the ROVs Bathysaurus (2008–2014; ARGUS remote Systems) and Ægir6000 (2015–2019; Kystdesign). Specimens from the Jan Mayen area were collected during the IceAGE project (Brix *et al*. 2014) and cruises with R/V *Håkon Mosby*, University of Bergen, headed by Torleiv Brattegard (Fig. 1). The map showing sample localities (Fig. 1) was created with QGIS ver. 3.22.4 (http://qgis.osgeo.org).

Morphological observations

All specimens were examined with a Leica M165 C stereo microscope and photographed with a Canon EOS 5D Mark II camera equipped with a 65 mm macro lens. Stacks of images were assembled with Zerene Stacker ver. 1.04 (https://www.zerenesystems.com). Some specimens were stained with a saturated solution of methylene blue in water to reveal potential staining patterns and/or a commercial solution of Shirlastain A to increase contrast. Parapodia were dissected and mounted on slides in glycerol, observed with an Olympus BX51 compound microscope equipped with DIC and photographed with a Canon EOS 600D Camera. Four specimens of *Caulleriella jormungandri* sp. nov. were examined and photographed with a Hitachi S-3400N scanning electron microscope (SEM). Specimens were first dehydrated in a series of baths from pure ethanol to pure HMDS, air dried, and then sputter-coated with gold. Two specimens of *Caulleriella jormungandri* and two specimens of *Raricirrus arcticus* were examined and photographed with a Zeiss SUPRA 55VP scanning electron microscope. Specimens were first dehydrated by Critical Point drying, then sputter coated with gold/palladium. Images and plates were edited with Gimp ver. 2.10.30 (https://www.gimp.org) and Inkscape ver. 1.2.1 (https://www.inkscape.org). All material, including the type specimens, is deposited in the University Museum of Bergen, University of Bergen (ZMBN, Norway) and in the Senckenberg Museum (SMF, Frankfurt, Germany). Due to the mounting system, several specimens used for SEM could not be recovered and are referred to in the paper by their BOLD processID. For these specimens, high-resolution pictures are available in BOLD and serve as digital vouchers.

In order to describe the morphology of the specimens in a precise, accurate and repeatable way, we use the following terms to describe the shape and proportions of the segments. The words "narrow/wide" are used to describe the width of a segment, from side to side. The words "short/long" describe the length of a segment, along the anteroposterior axis. The word "high" is used to describe the height of a segment, along the dorsoventral axis.

Taxon sampling for the molecular phylogenetic analyses

New sequences were produced for 17 specimens of *Caulleriella jormungandri* sp. nov. and five specimens of *Raricirrus arcticus*. We also included the newly obtained sequences of two species identified as *Caulleriella* sp. 18 and *Caulleriella* sp. 43, as well as *Raricirrus beryli* Petersen & George, 1991, *Dodecaceria concharum* Örsted, 1843, *Chaetozone quinta* Grosse, Capa & Bakken, 2021, *Chaetozone setosa* Malmgren, 1867, *Tharyx killariensis* (Southern, 1914), *Tharyx robustus* Blake & Göransson, 2015 and two species identified as *Aphelochaeta* sp. B and *Aphelochaeta* sp. N. The sequences of two more species of *Raricirrus*, *R. anubis* Jimi, Fujimoto, Fujiwara, Oguchi & Miura, 2022 and *R. jennae* Magalhães, Linse & Wiklund, 2017, were obtained from GenBank (for voucher numbers see Supp. file 1). These sequences were linked to recent publications with detailed species descriptions ensuring their reliable taxonomic identification. Two representatives of Flabelligeridae de Saint-Joseph, 1894 were chosen as outgroups (Supp. file 1).

DNA sequencing

A few tentacles and/or branchiae, parapodia, middle or posterior segments were taken from the 96% ethanol-fixed specimens for molecular analyses. Tissues were placed in 50 µL of QuickExtract (Lucigen) and incubated at 65°C for one to five hours then at 95°C for five minutes or extracted with the QIAGEN DNeasy Blood & Tissue kit following the manufacturer's protocol. PCR mixes contained 10 µL of
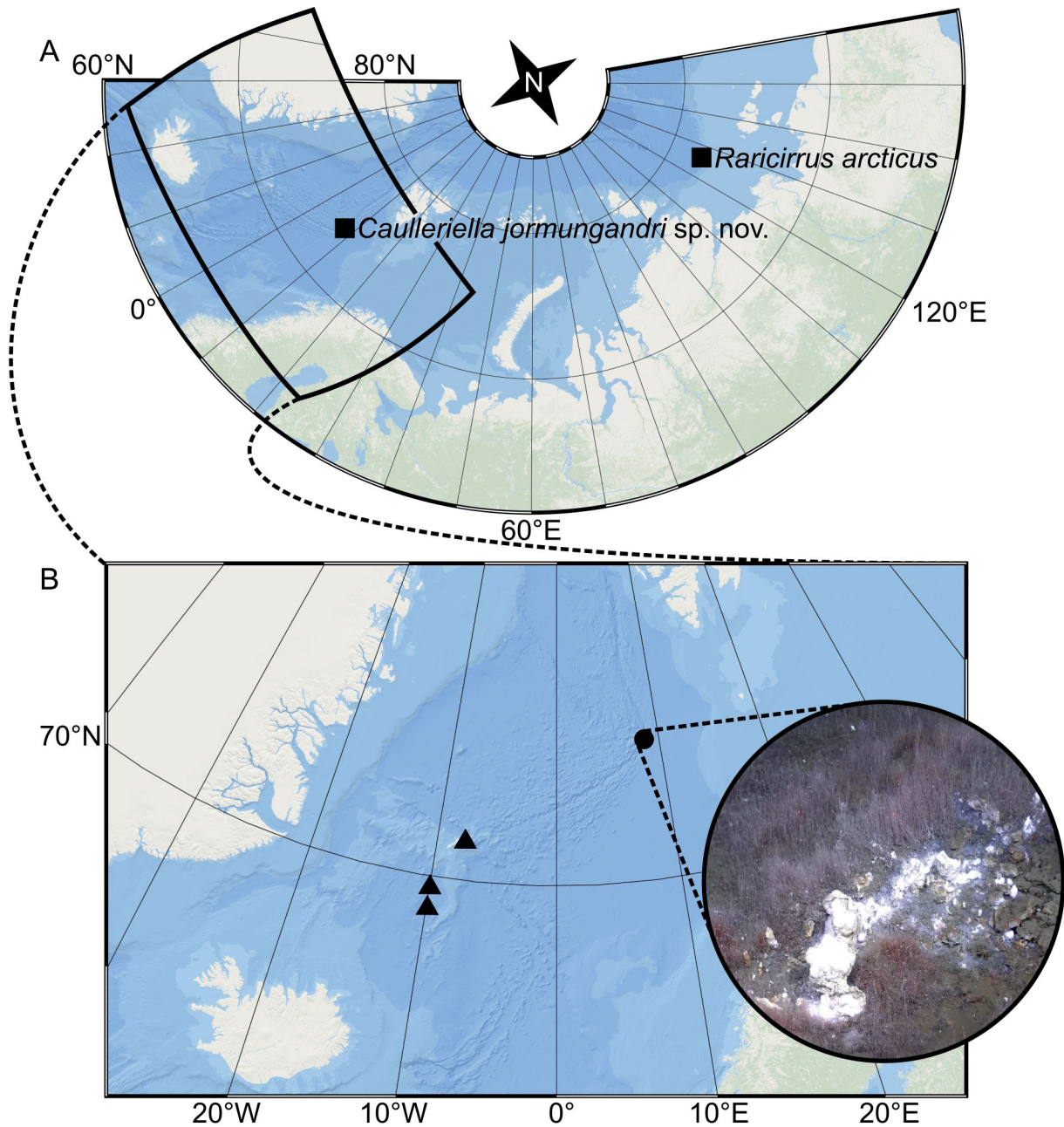

Fig. 1. Distribution and sampling. **A**. Type localities of *Caulleriella jormungandri* sp. nov. and *Raricirrus arcticus* Buzhinskaja & Smirnov, 2017 (black squares) and study area. **B**. Study area with station locations: the black circle indicates the position of LCVF where both species were found, black triangles indicate additional locations where *C. jormungandri* was found; the insert shows the Barite Field diffuse venting area of the field, with dense worm forests formed by the siboglinid *Sclerolinum contortum* Smirnov, 2000. Image credit: Center for Deep Sea Research, University of Bergen.

RedTaq 1.1x MasterMix 2.0 mM $MgCl_2$ (VWR), 0.30 μL of each primer and 1.4 μL of DNA template for a final reaction volume of 12 μL, or alternatively with 2.5 μL CoralLoad buffer (QIAGEN), 1 μL MgCl (QIAGEN, 25 mM), 2 μL dNTP (TaKaRa, 2.5 mM of each dNTP), 1 μL of each of the primers (10 μM solution), 0.15 mL TaKaRa HS Taq, 1 or 2 μL DNA extraction and ddH2O to make the total reaction volume 25 μL. COI was amplified using the primer pairs HCO/LCO (Folmer *et al.* 1994), jgLCO/jgHCO (Geller *et al.* 2013) or polyLCO/polyHCO (Carr *et al.* 2011), 16S was amplified using the primer pair 16Sarl/16SbrH (Palumbi *et al.* 1996), and the D1-D2 region of 28S was amplified using the primer pair 28SC1/28SD2 (Le *et al.* 1993) or 28F5 (Passamaneck *et al.* 2004) and Po28R4 (Struck *et al.* 2006) (primer sequences and PCR protocols are available in Supp. file 5). PCR products were run on a 1% agarose gel to check reaction success. Successful PCR products were purified and sequenced on both strands by Eurofins Genomics (Germany) or prepared with BigDye ver. 3.1 (Life Technologies) and run on an Automatic Sequencer 3730XL at the sequencing facility of the Department of Biological Sciences, University of Bergen. Forward and reverse reads were merged into consensus sequences using Geneious Pro ver. 5.4.6 (https://geneious.com). BOLD processID and GeneBank accession numbers are available in Supp file 1.

Phylogenetic analyses

Four different datasets were assembled. Three contained respectively COI, 16S and 28S sequences obtained for this study as well as available sequences of relevant specimens of the family Cirratulidae and two outgroups. The fourth dataset was created by concatenating the first three in Geneious Pro ver. 5.4.6. for a combined analysis.

COI sequences were aligned using MUSCLE (Edgard 2004) implemented in Aliview ver. 1.25 (Larsson 2014). 16S and 28S sequences were aligned using MAFFT 7 online version (Katoh *et al.* 2017) as it handles gappy alignments more accurately. Alignments are available in Supp. file 2. Pairwise distances using the HKY substitution model were calculated in Geneious Pro ver. 5.4.6. Maximum Likelihood (ML) analyses were performed with IQ-TREE ver. 2 (Minh *et al.* 2020) using ModelFinder for model selection (Kalyaanamoorthy *et al.* 2017) with 10000 ultrafast bootstraps (Hoang *et al.* 2018). For the concatenated datasets, the TESTMERGE option was used and partitions were allowed to have different speeds. Analyses were run on CIPRES Science Gateway (Miller *et al.* 2010). Trees were visualised in Interactive Tree of Life (iTOL) ver. 6.7 (Letunic & Bork 2021).

Abbreviations

br1 = first branchia
br2 = second branchia
ch1 = first chaetiger
ch2 = second chaetiger
dT = dorsal tentacle
mo = mouth
nuO = nuchal organ
per = peristomium
pr = prostomium
pyg = pygidium

Results

Phylogeny

The resulting concatenated matrix consisted of 2347 nucleotides with 1014 variable and 797 parsimony informative sites. *Caulleriella* and *Raricirrus* formed highly supported monophyletic groups (BP 100). *Raricirrus* was recovered as sister to *Dodecaceria* (BP 100). *Caulleriella* formed a clade with the two

species of *Chaetozone* (BP 70) although the latter was not monophyletic (Fig. 2). The COI tree topology was identical to the tree based on the concatenated matrix. The 16S analysis differed in the position of *Dodecaceria/Raricirrus* clade which was nested within the *Caulleriella/Chaetozone* clade (BP 81). In the 28S analysis, the *Tharyx/Aphelochaeta* clade was sister to the *Chaetozone/Caulleriella* clade (BP 76).

Intraspecific genetic distances within *Caulleriella jormungandri* sp. nov. (HKY model of substitution) were 0.7% maximum in COI, 0.2% maximum in 16S, and 0% in 28S. The minimum distances with its
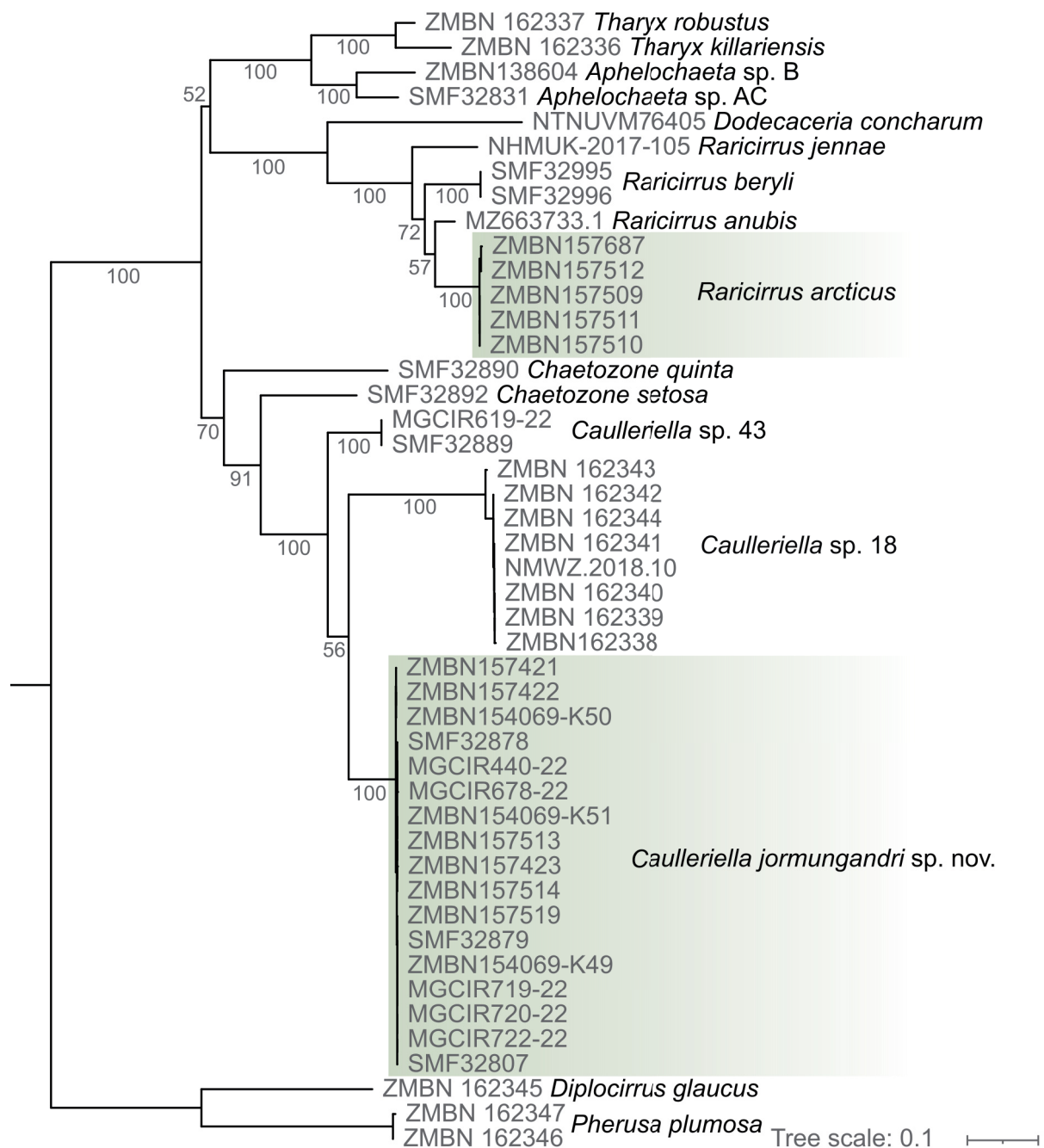
Fig. 2. ML phylogenetic tree based on the combined dataset of COI, 16S and 28S. Bootstrap values are indicated under or above branches.

nearest neighbour, *Caulleriella* sp. 43 was 21.9% in COI, 18.1% in 16S, and 4.4% in 28S. *Raricirrus arcticus* was consistently recovered very distant from *R. beryli*, the only other species of the genus reported from the Nordic seas, with minimum interspecific distances of 21.6% in COI, 7% in 16S, and 9.1% in 28S. Distance matrices and gene trees are respectively available in Supp. file 3 and Supp. file 4.

Taxonomy

Phylum *Annelida* Lamarck, 1809
Subclass *Sedentaria* Lamarck, 1818
Family *Cirratulidae* Ryckholdt, 1851

Genus ***Caulleriella*** Chamberlin, 1919

Type species

Cirratulus viridis Langerhans, 1880. Original designation by Chamberlin (1919).

Diagnosis (after Blake 2021)

Prostomium elongate, conical to pointed; peristomium elongated to short, dorsal tentacles usually beginning anterior to chaetiger 1. Middle body segments not beaded; parapodia often with noto- and neuropodia widely separated laterally. Chaetae including capillaries and bidentate, crotchet-like hooks, not arranged into modified cinctures. In some species, unidentate hooks may occur in some regions of body in addition to bidentate hooks. Pygidium either simple conical lobe or with one or two anal cirri.

Caulleriella jormungandri sp. nov.
urn:lsid:zoobank.org:act:FF0D1D4D-39A7-48ED-A5DD-E457E1A47D20
Figs 3–7

Diagnosis

Body long and slender, not threadlike, posteriorly flattened; three peristomial rings, first segment chaetigerous; 3–6 bidentate spines per neuropodium from chaetiger 4, 3–4 per notopodium from chaetiger 16.

Etymology

In Norse mythology, Jörmungandr is a sea serpent or worm and a child of Loki. As a marine worm discovered in the Loki's Castle vent field, *Caulleriella jormungandri* sp. nov. is named after this mythological creature.

Material examined

Holotype
ARCTIC MID-OCEAN RIDGE • Loki's Castle hydrothermal vent field; 73.56633° N, 8.15946° E; 2350 m depth; 11 Jul. 2015; collected by ROV; sample GS15-AGR09; fixed in 96% ethanol; DNA-voucher: CaH03; ZMBN 157421.

Paratypes
ARCTIC MID-OCEAN RIDGE • 1 spec.; Loki's Castle hydrothermal vent field; 73.5662° N, 8.1585° E; 2300 m depth; 14 Jul. 2008; collected by ROV; sample BIODEEP08-LC-ROV11; fixed in 96% ethanol; ZMBN 157515 • 1 spec.; Loki's Castle hydrothermal vent field, Barite Field; 74.5661° N, 8.1585° E; 2357 m depth; 7 Aug. 2009; collected by ROV; sample H2DEEP09-ROV08; fixed in 96% ethanol; ZMBN 157516 • 1 spec.; same data as for preceding; DNA-voucher: LC01; ZMBN 157517 • 1 spec.; same data as for preceding; DNA-voucher: LC04; ZMBN 157518 • 1 spec.; same data as for preceding;

ZMBN 157520 • 1 spec.; same data as for preceding; DNA-voucher: LC02; ZMBN 157513 • 1 spec.; same data as for preceding; DNA-voucher: LC03; ZMBN 157514 • 1 spec.; same data as for preceding; DNA-voucher: LC05; ZMBN 157519 • 3 specs; same data as for preceding; mounted on SEM-stubs; ZMBN 157681 to 157683 • 1 spec.; Loki's Castle hydrothermal vent field; 73.5662° N, 8.1610° E; 2335 m depth; 17 Jul. 2010; collected by ROV; sample GS10-ROV06-b; fixed in 96% ethanol; ZMBN 157521 • 1 spec.; same data as for preceding; 73.5668° N, 8.1605° E; 2373 m depth; 19 Jul. 2010; collected by ROV; sample GS10-ROV10; fixed in 96% ethanol; ZMBN 157522 • 109 specs; same data as for preceding; 73.5663° N, 8.1610° E; 2350 m depth; 11 Jul. 2015; collected by ROV; sample GS15-AGR09; fixed in 96% ethanol; ZMBN 154069 • 3 specs; same data as for preceding; DNA vouchers: K49, K50, K51; no repository (specimens used for DNA) • 1 spec.; same data as for preceding; DNA-voucher: CaH01; ZMBN 157419 • 1 spec.; same data as for preceding; DNA-voucher: CaH02; ZMBN 157420 • 1 spec.; same data as for preceding; DNA-voucher: CaH04; ZMBN 157422 • 1 spec.; same data as for preceding; DNA-voucher: CaH05; ZMBN 157423 • 1 spec.; Loki's Castle hydrothermal vent field, barite field; 73.5664° N, 8.1618° E; 2342 m depth; 10 Jul. 2017; collected by ROV; sample GS17-ROV18-SS4; fixed in 96% ethanol; ZMBN 157524 • 8 specs; Loki's Castle hydrothermal vent field, barite field, chimney; 73.5666° N, 8.1624° E; 2344 m depth; 12 Jul. 2017; collected by ROV; sample GS17-ROV21-R1; fixed in 96% ethanol; ZMBN 157523 • 2 specs; Loki's Castle hydrothermal vent field, barite field, worm forest; 73.5663° N, 8.1624° E; 2342 m depth; 18 Jul. 2018; collected by ROV; sample GS18-107-ROV26; fixed in 96% ethanol; ZMBN 157597 • 1 spec.; same data as for preceding; ZMBN 157598 • 2 specs; same locality as for preceding; 73.5662° N, 8.1621° E; 2341 m depth; 22 Jul. 2018; collected by ROV; GS18-107-ROV28; fixed in 96% ethanol; ZMBN 157599 • 1 spec.; Loki's Castle hydrothermal vent field, oasis, worm forest; 73.5671° N, 8.1617° E; 2356 m depth; 1 Jul. 2019; collected by ROV; GS19-108-ROV25; fixed in 96% ethanol; ZMBN 138216 • 7 specs; same data as for preceding; fixed in 96% ethanol; ZMBN 138212.

Other material

ARCTIC MID-OCEAN RIDGE • 37 specs; 68.70600° N, 11.61100° W; 1811 m depth; 16 Mar. 1984; collected by dredge; sample HM84.03.16-2; fixed in formaldehyde and transferred to 75% ethanol; ZMBN 144543 • 6 specs; 69.60600° N, 9.91000° W; 2212 m depth; 26 Jul. 1986; collected by dredge; sample HM86.07.26-1; fixed in formaldehyde and transferred to 75% ethanol; ZMBN 157644 • 1 spec.; 69.10616° N, 9.9120° W; 2174–2204 m depth; 17 Sep. 2011; sample M85-3-1155; fixed in 96% ethanol; DNA-voucher: MG1000; SMF 32807 • 1 spec.; same data as for preceding; DNA-voucher: MG1001; no repository (specimen used for SEM) • 1 spec.; 69.103° N, 9.9225° W; 2169–2172 m depth; 17 Sep. 2011; collected with Agassiz trawl; sample M85-3-1160; fixed in 96% ethanol; DNA-voucher: MG763 no repository (specimen used for SEM) • 1 spec.; 71.1110° N, 7.92933° W; 2160–2203 m depth; 17 Sep. 2011; fixed in 96% ethanol; collected with epibenthic sledge; sample M85-3-1159; DNA-voucher: MG1041; SMF 32878 • 1 spec.; same data as for preceding; DNA-voucher: MG1042 no repository (specimen used for SEM) • 1 spec.; same data as for preceding; DNA-voucher: MG1043 no repository (specimen used for SEM) • 1 spec.; same data as for preceding; DNA-voucher: MG1044; SMF 32879 • 1 spec.; same data as for preceding; DNA-voucher: MG1045; SMF 32880.

Description

Holotype complete, 12 mm long, 0.7 mm wide, 72 segments. Other complete specimens ranging 3–12 mm in length and 0.2–0.7 mm in width for 47–77 segments. Colour in ethanol light tan to brown, rarely dark grey (Figs 3–4). Body long and slender, without any distinct enlargement, cylindrical in cross section in anterior and middle body, dorsoventrally flattened in posterior region (Figs 3–4). Anterior 8–13 segments 3–4 times wider and higher than long, round in cross section, lengthening to 2–3 times wider and higher than long in midbody. Posterior 20 segments 4–5 times wider and 2 times higher than long, oval to rectangular in cross section. Dorsal groove or ridge absent. Thin ventral groove accompanied by dark line sometimes present, depending on fixation.

Prostomium half to two thirds as long as peristomium, conical, rounded on anterior margin, without rings; eyespots absent (Figs 5A–C, F, 6B–C); nuchal organs simple round slits at posterior lateral margins (Fig. 5C–E). Peristomium as long as 3–4 anterior segments, as high and wide as long, with three distinct rings of similar length, anterior ring overlapping prostomium dorsally, middle ring overlapping posterior ring dorsally between tentacles, posterior ring partially fused to chaetiger 1. Dorsal tentacles arising from third peristomial ring, well separated from one another and anterior to first pair of branchiae (Figs 5A–C, F, 6B–C). First pair of branchiae arising between posterior margin of peristomium and first segment postero-lateral to tentacles. Second pair of branchiae arising from chaetiger 1, dorsal and slightly posterior to parapodia (Fig. 5A–B, F). Subsequent branchiae similarly placed, present only in anterior part of body.

Parapodia biramous, neuropodia and notopodia well separated, notopodia forming low shoulders in anterior chaetigers, neuropodia lateral anteriorly and nearly reaching ventral position in posterior chaetigers. Capillary chaetae 8–10 per neuropodium and notopodium from chaetiger 1, decreasing
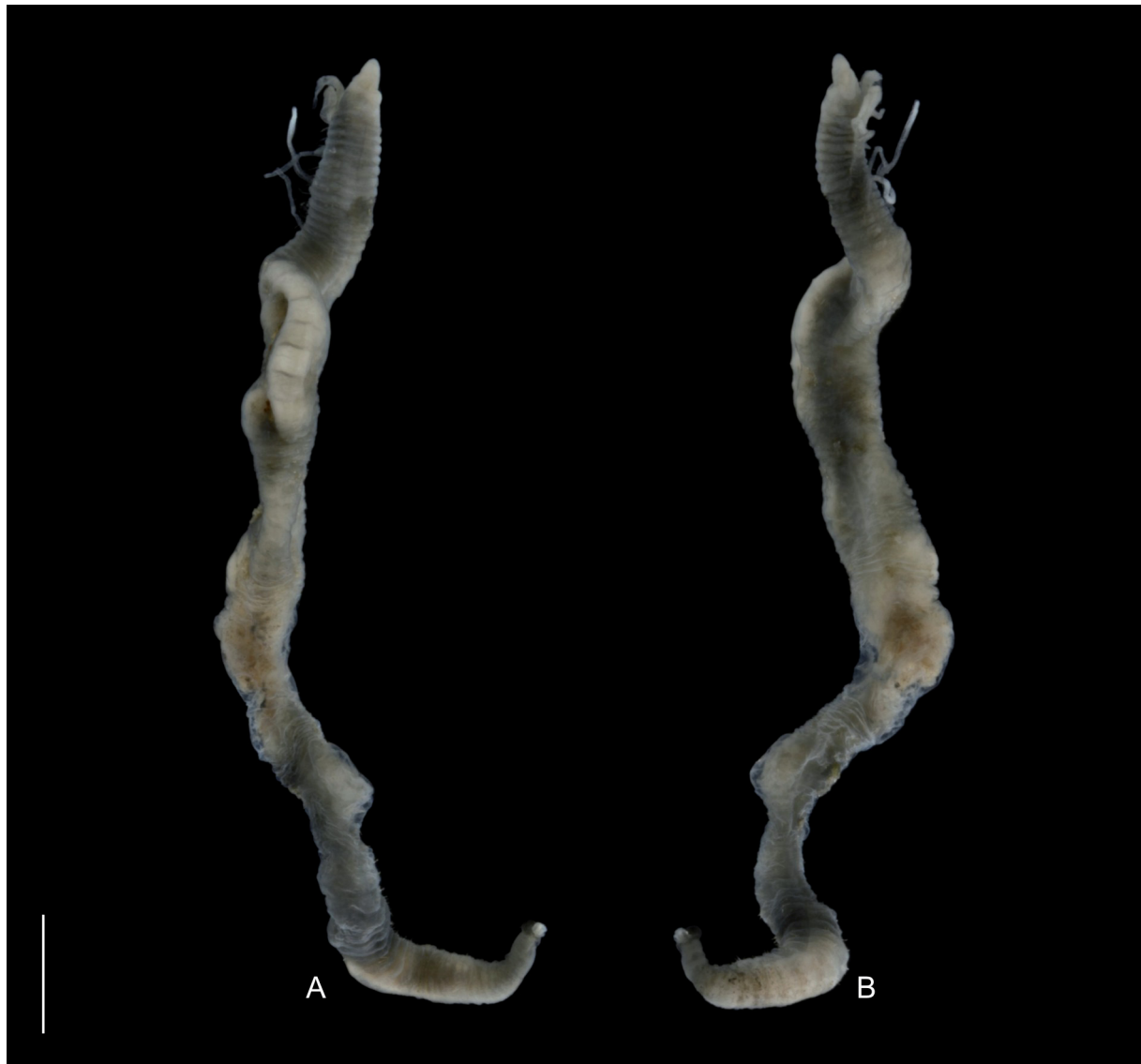

Fig. 3. *Caulleriella jormungandri* sp. nov., holotype (ZMBN 157421). **A**. Dorsolateral view. **B**. Ventrolateral view. Scale bar = 1 mm.

Fig. 4. *Caulleriella jormungandri* sp. nov., complete specimens. **A**. DNA voucher. **B–H**. Paratypes. **A**. DNA voucher MG1043 (no repository, specimen used for SEM). **B**. SMF 32878. **C**. SMF 32879. **D**. SMF 32880. **E–G**. ZMBN 157520. **H**. ZMBN 157516. Scale bar = 1 mm.
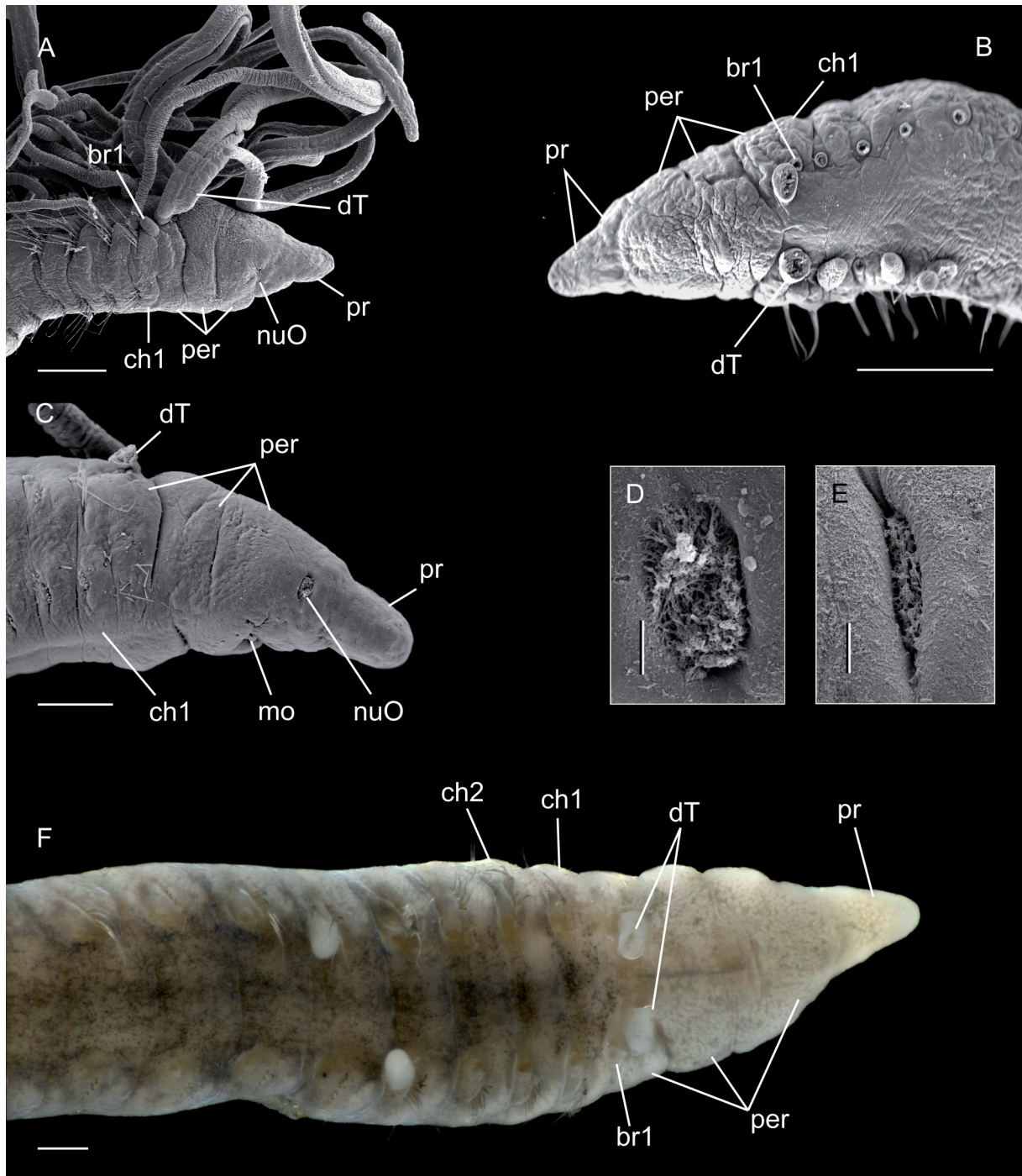
Fig. 5. *Caulleriella jormungandri* sp. nov., anterior morphology. **A**. Paratype ZMBN 157681. **B**. DNA voucher MG1043 (no repository, specimen used for SEM). **C–D**. DNA voucher MG763 (no repository, specimen used for SEM). **E**. DNA voucher MG1042 (no repository, specimen used for SEM). **F**. Paratype ZMBN 157520. **A, C**. Anterior end in lateral view. **B, F**. Anterior end in dorsal view. **D–E**. Nuchal organs. Abbreviations: br1 = first branchia; ch1 = first chaetiger; ch2 = second chaetiger; dT = dorsal tentacle; mo = mouth; nuO = nuchal organ; per = peristomium; pr = prostomium. Scale bars: A = 200 μm; B = 250 μm; C, F = 100 μm; D–E = 10 μm.
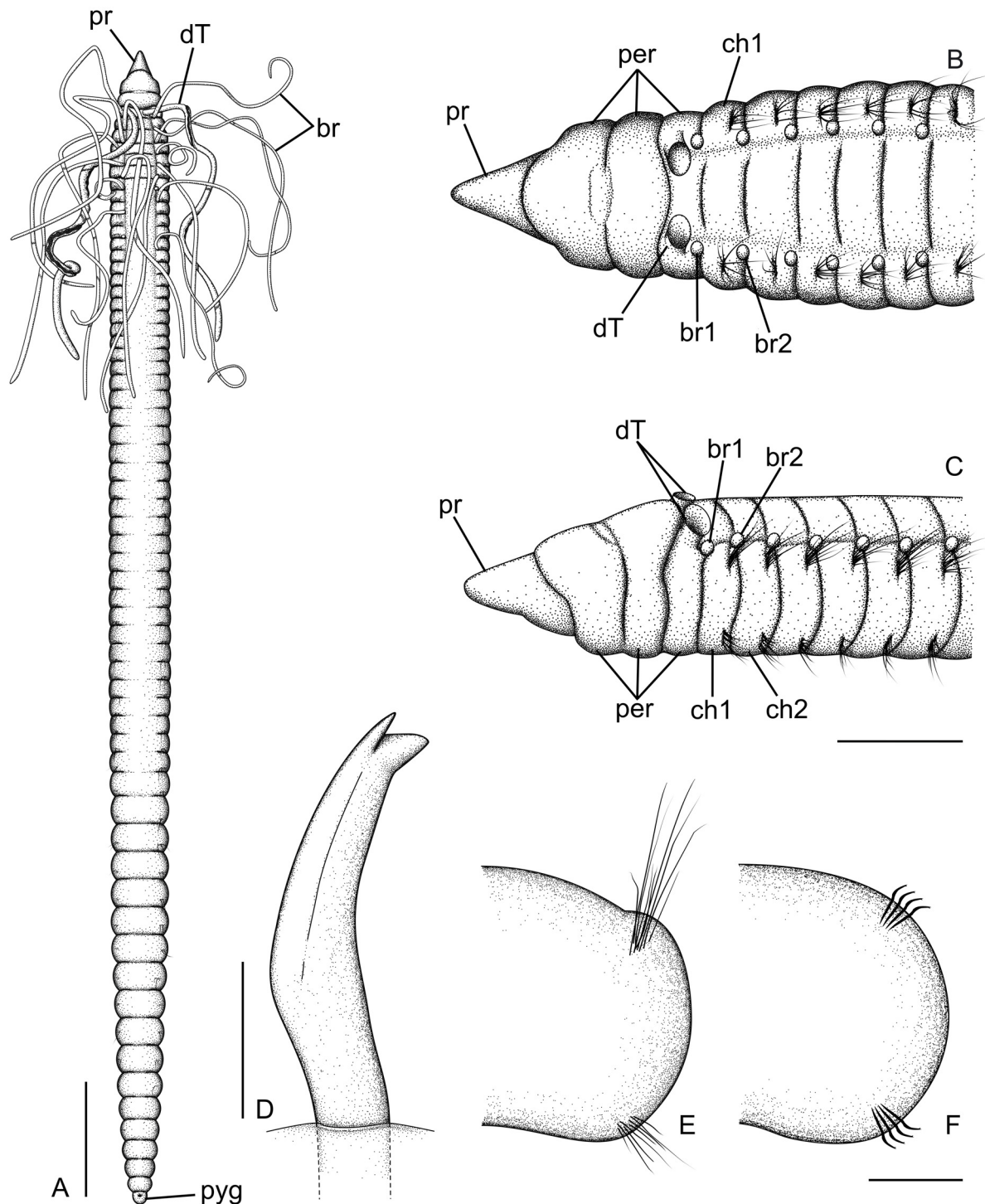
Fig. 6. *Caulleriella jormungandri* sp. nov., schematic representation. **A**. Complete specimen, dorsal view. **B**. Anterior end, dorsal view. **C**. Anterior end, lateral view. **D**. Bidentate spine. **E**. Cross section of anterior segment. **F**. Cross section of posterior segment. Abbreviations: br = branchiae; br1 = first branchia; br2 = second branchia; ch1 = first chaetiger; ch2 = second chaetiger; dT = dorsal tentacle; per = peristomium; pr = prostomium; pyg = pygidium. Scale bars: A = 1 mm; B–C = 250 μm; D = 10 μm; E–F = 200 μm.

in number posteriorly; finely fibrillated along one edge (Fig. 7A–B). On neuropodia and notopodia without spines, capillary chaetae are arranged in two rows, posterior capillaries twice as long as anterior ones (Fig. 7A). Bidentate spines from chaetiger 4, 3–6 per neuropodium; from chaetiger 16, 3–4 per notopodium; long, relatively thick, slightly curved with basal shoulder, main fang thick, pointed, at 45° angle from shaft, apical tooth short, pointed, in prolongation of alate flange on convex side of shaft (Fig. 7C–G). Companion capillaries arise between most spines.

Pygidium with terminal anus and rounded ventral lobe (Fig. 6A).

Methylene blue staining pattern

The entire body retains a light blue colour with dark blue circles around neuropodia and notopodia anteriorly. Some dark intersegmental ventral bands are sometimes visible on the first few segments.

Comparative remarks

At present, nine species of *Caulleriella* have been reported from depths over 500 m (Blake 2021), including the new species described in the present paper. One species is known from the Pacific Ocean, four from the Southern Ocean and four from the Atlantic Ocean. *Caulleriella jormungandri* sp. nov. is
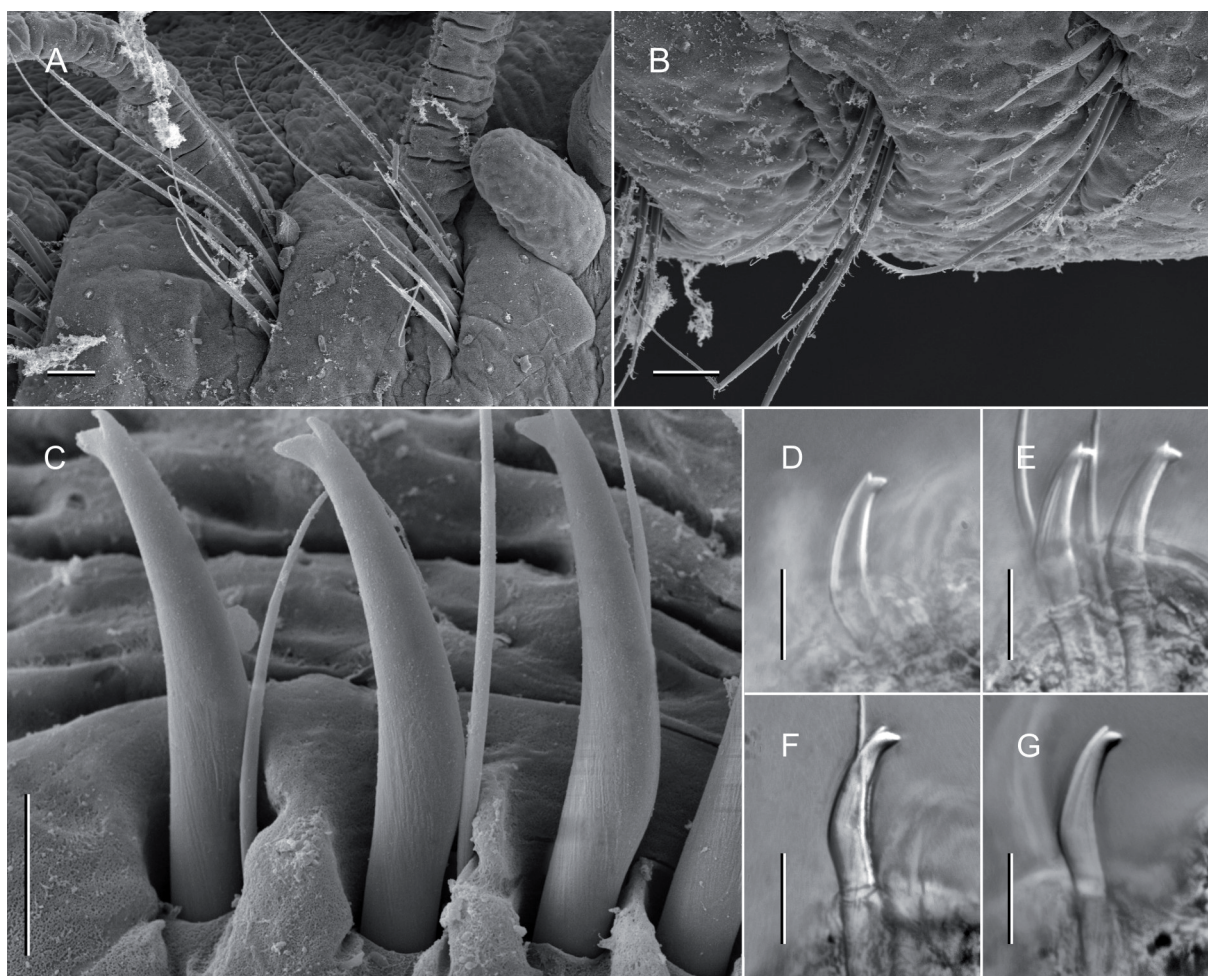

Fig. 7. *Caulleriella jormungandri* sp. nov., chaetae morphology. **A–B**. Paratype ZMBN 157681. **D–G**. Paratype SMF 32807. **A**. First three notopodia. **B**. First three neuropodia. **C**. Paratype (MG1043), neuropodial spines. **D–G**. Neuropodial spines. Scale bars: A–B = 20 µm; C = 10 µm; D–G = 20 µm.

most similar to *C. eltaninae* Blake, 2018 and *C. kacyae* Blake, 2018 from the Southern Ocean in having three peristomial rings. *Caulleriella jormungandri* differs from *C. eltaninae* in that the first segment is the first chaetiger (achaetous in *C. eltaninae*), in the presence of notopodial spines and in the lack of pygidial cirri. *Caulleriella jormungandri* mainly differs from *C. kacyae* by the lack of pygidial cirri and the number and distribution of spines in neuropodia (up to 6 from segment 4 in the former vs up to 6 from segment 18 in the latter) and notopodia (up to 4 from segment 16 in the former vs up to 2 from segment 105 in the latter). *Caulleriella jormungandri* is easily distinguished from other deep-sea North Atlantic species (*Caulleriella filliformia* Blake, 2021, *Caulleriella pintada* Blake, 2021 and *Caulleriella rodmani* Blake, 2021) by the body shape and the peristomium, as all these other species have threadlike bodies and a single peristomial ring.

Distribution and habitat

Caulleriella jormungandri sp. nov. is a common species at Loki's Castle vent site in areas with low-temperature diffuse venting, where it is found in association with dense aggregations of other polychaetes (worm forest), in particular *Sclerolinum contortum* and *Nicomache lokii*. Additional specimens were collected from five localities close to Jan Mayen in depths between 1800 and 2200 m (Fig. 1). No indication of hydrothermal activity was recorded from the localities near Jan Mayen, suggesting that *Caulleriella jormungandri* is not strictly associated with hydrothermal environments.

<div align="center">Genus Raricirrus Hartman, 1961</div>

Type species

Raricirrus maculatus Hartman, 1961. Original designation.

Diagnosis (after Magalhães *et al.* 2017)

Prostomium rounded, eyes absent, nuchal organs shallow ciliary pits, postero-lateral, rounded or elongate. Peristomium not obviously delimited from prostomium and chaetiger 1 dorsally; ventral cilia may be present on peristomium and first few segments; first segment complete chaetiger. Tentacles absent. Branchiae present on several segments, filiform or club-like distally. Notochaetae short and long serrate capillaries anteriorly and modified chaetae posteriorly as acicular spines, coarsely serrate forms and short pectinate falcigers. Neurochaetae short serrate capillaries and/or modified chaetae such as acicular spines, falcate and finely pectinate, and coarsely serrate chaetae. Simple enlarged spines may be present in one or two posterior end segments. Heart body enlarged dorsal vessel present in variable number of anterior and middle segments. Pygidium simple lobe, anal aperture usually dorsal; posterior region distinct with few segments wider than preceding ones. Asexual reproduction via architomy. Sexual reproduction may occur; epitoke individuals, hermaphroditism, seminal vesicle and reproductive stylet may be present.

<div align="center">Raricirrus arcticus Buzhinskaja & Smirnov, 2017
Figs 8–9</div>

Diagnosis

Heart body from chaetiger 2; branchiae cylindrical; distinct ciliary field near mouth; long serrate chaetae with straight tips in midbody neuropodia.

Material examined

ARCTIC MID-OCEAN RIDGE • 1 spec.; Loki's Castle hydrothermal vent field; 73.5662° N, 8.1585° E; 2300 m depth; 14 Jul. 2008; collected with ROV; sample BIODEEP08-LC-ROV11; fixed in 96% ethanol; DNA voucher: LC06; ZMBN 157600 • 5 specs; same data as for preceding; ZMBN 157689 • 3 specs;

Loki's Castle hydrothermal vent field; 73.5662° N, 8.1583° E; 2330 m depth; 15 Jul. 2008; collected with ROV; sample BIODEEP08-LC-ROV12; fixed in 96% ethanol; ZMBN 157601 • 17 specs; Loki's Castle hydrothermal vent field, barite field; 74.5661° N, 8.1585° E; 2357 m depth; 7 Aug. 2009; collected with ROV; sample H2DEEP09-ROV08; fixed in 96% ethanol; ZMBN 157686 • 72 specs; same data as for preceding; ZMBN 157602 • 1 spec.; same data as for preceding; DNA-voucher: LC08; ZMBN 157621 • 1 spec.; same data as for preceding; DNA-voucher: LC09; ZMBN 157687 • 4 specs; same data as for preceding; ZMBN 157688 • 1 spec.; same data as for preceding; ZMBN 157604 • 5 specs; same data as for preceding; ZMBN 157610 • 1 spec.; same data as for preceding; ZMBN 157605 • 2 specs; same data as for preceding; mounted on SEM-stub; ZMBN 157685 • 1 spec.; same data as for preceding; ZMBN 157603 • 1 spec.; Loki's Castle hydrothermal vent field, barite field; 73.5665° N, 8.1618° E; 2385 m depth; 15 Jul. 2010; collected with ROV; sample GS10-ROV04; fixed in 96% ethanol; DNA-voucher: LC07; ZMBN 157509 • 1 spec.; same data as for preceding; DNA-voucher: LC10; ZMBN 157510 • 1 spec.; same data as for preceding; DNA-voucher: LC11; ZMBN 157511 • 24 specs; same data as for preceding; ZMBN 157606 • 28 specs; same data as for preceding; ZMBN 157607 • 46 specs; same data as for preceding; fixed in formaldehyde and transferred to 75% ethanol; ZMBN 157608 • 2 specs; Loki's Castle hydrothermal vent field; 73.5673° N, 8.1573° E; 2314 m depth; 17 Jul. 2010; collected with ROV; sample GS10-ROV07; fixed in 96% ethanol; ZMBN 157611 • 1 spec.; same data as for preceding; mounted on SEM-stub; ZMBN 157684 • 4 specs; Loki's Castle hydrothermal vent field; 73.5662° N, 8.1610° E; 2335 m depth; 17 Jul. 2010; collected with ROV; sample GS10-ROV06-b; fixed in 96% ethanol; ZMBN 157609 • 5 specs; Loki's Castle hydrothermal vent field, eastern mound, Joao; 73.5658° N, 8.1610° E; 2385 m depth; 18 Jul. 2010; collected with ROV; sample GS10-ROV09; fixed in formaldehyde and transferred to 75% ethanol; ZMBN 157622 • 1 spec.; same data as for preceding; fixed in 96% ethanol; DNA-voucher: LC12; ZMBN 157512 • 14 specs; same data as for preceding; fixed in 96% ethanol; ZMBN 157612 • 1 spec.; Loki's Castle hydrothermal vent field; 73.5668° N, 8.1605° E; 2373 m depth; 19 Jul. 2010; fixed in 96% ethanol; DNA voucher: LC13; ZMBN 157613 • 2 specs; Loki's Castle hydrothermal vent field; 73.5663° N, 8.1610° E; 2350 m depth; 11 Jul. 2015; collected with ROV; sample GS10-ROV10; fixed in 96% ethanol; ZMBN 157614 • 4 specs; Loki's Castle hydrothermal vent field, barite field; 73.5664° N, 8.1618° E; 2342 m depth; 10 Jul. 2017; fixed in 96% ethanol; ZMBN 157617 • 3 specs; Loki's Castle hydrothermal vent field, eastern mound, base of chimney; 73.5664° N, 8.1616° E; 2329 m depth; 11 Jul. 2017; collected with ROV; sample GS15-AGR09; fixed in 96% ethanol; ZMBN 157645 • 6 specs; same data as for preceding; ZMBN 157616 • 5 specs; Loki's Castle hydrothermal vent field, barite field, chimney; 73.5666° N, 8.1624° E; 2344 m depth; 12 Jul. 2017; collected with ROV; sample GS17-ROV21-R1; fixed in 96% ethanol; ZMBN 157615 • 1 spec.; Loki's Castle hydrothermal vent field, barite field, worm forest; 73.5663° N, 8.1624° E; 2342 m depth; 18 Jul. 2018; collected with ROV; sample GS18-107-ROV26; fixed in 96% ethanol; ZMBN 157619 • 1 spec.; same data as for preceding; ZMBN 157620 • 4 specs; Loki's Castle hydrothermal vent field, barite field, worm forest; 73.5662° N, 8.1621° E; 2341 m depth; 22 Jul. 2018; collected by ROV; sample GS18-107-ROV28; fixed in 96% ethanol; ZMBN 157451 • 2 specs; Loki's Castle hydrothermal vent field, barite field, worm forest; 73.5665° N, 8.1623° E; 2342 m depth; 26 Jun. 2019; collected with ROV; sample GS19-108-ROV19; fixed in 96% ethanol; ZMBN 147555 • 2 specs; same data as for preceding; 73.5664° N, 8.1623° E; 2345 m depth; 29 Jun. 2019; collected with ROV; sample GS19-108-ROV22; fixed in 96% ethanol; ZMBN 138221 • 2 specs; same data as for preceding; ZMBN 138223 • 2 specs; Loki's Castle hydrothermal vent field, oasis, worm forest; 73.5671° N, 8.1617° E; 2356 m depth; 1 Jul. 2019; collected with ROV; sample GS19-108-ROV25; fixed in 96% ethanol; ZMBN 138217 • 1 spec.; same data as for preceding; ZMBN 138218 • 15 specs; Loki's Castle hydrothermal vent field, oasis, worm forest; 73.567° N, 8.1617° E; 2356 m depth; 14 Jul. 2022; collected with ROV; sample GS22-108-ROV575; fixed in 96% ethanol; ZMBN 157500 • 1 spec.; Loki's Castle hydrothermal vent field, eastern mound, base of chimney; 73.5664° N, 8.16° E; 2313 m depth; 10 Jul. 2017; collected with ROV; sample GS17-ROV18-SS5; fixed in 96% ethanol; ZMBN 157618.

Description

Complete specimens 5–8 mm long and 0.2–0.9 mm wide for 27–35 segments. Colour in ethanol dark brown to black, rarely light tan. Wide and convoluted dark heart body distinctly visible from segment 11–12 to 16–18. Body short, anterior and median chaetigers bead-shaped, transitioning in posterior half or third in distinct flattened region with short and wide segments. Anterior and middle segments twice as high and wide as long, or up to as wide and high as long; posterior segments up to four times wider and three times higher than long. Dorsal groove or ridge absent. Ventral ridge present along posterior part of body (Fig. 8). Large portion of individuals regenerating anterior or posterior parts of body.

Prostomium short, rounded, dorsoventrally flattened; nuchal organs large rounded ciliary fields at posterior dorsolateral margins connected by transversal ventral ciliary bands. Peristomium short, fused with chaetiger 1 in single ovoid bead, with ventral groove separating them; ciliary field present ventrally, continuing as longitudinal band through several anterior segments (Fig. 9B). Branchiae arising from posterior segmental margins, slightly above notopodia, present as early as segment 6 and as far as segment 16.

Fig. 8. *Raricirrus arcticus* Buzhinskaja & Smirnov, 2017, complete specimens. **A, F**. ZMBN 157688. **B–C**. ZMBN 157689. **D–E, G**. ZMBN 157686. **H**. ZMBN 157685. Scale bar = 1 mm.
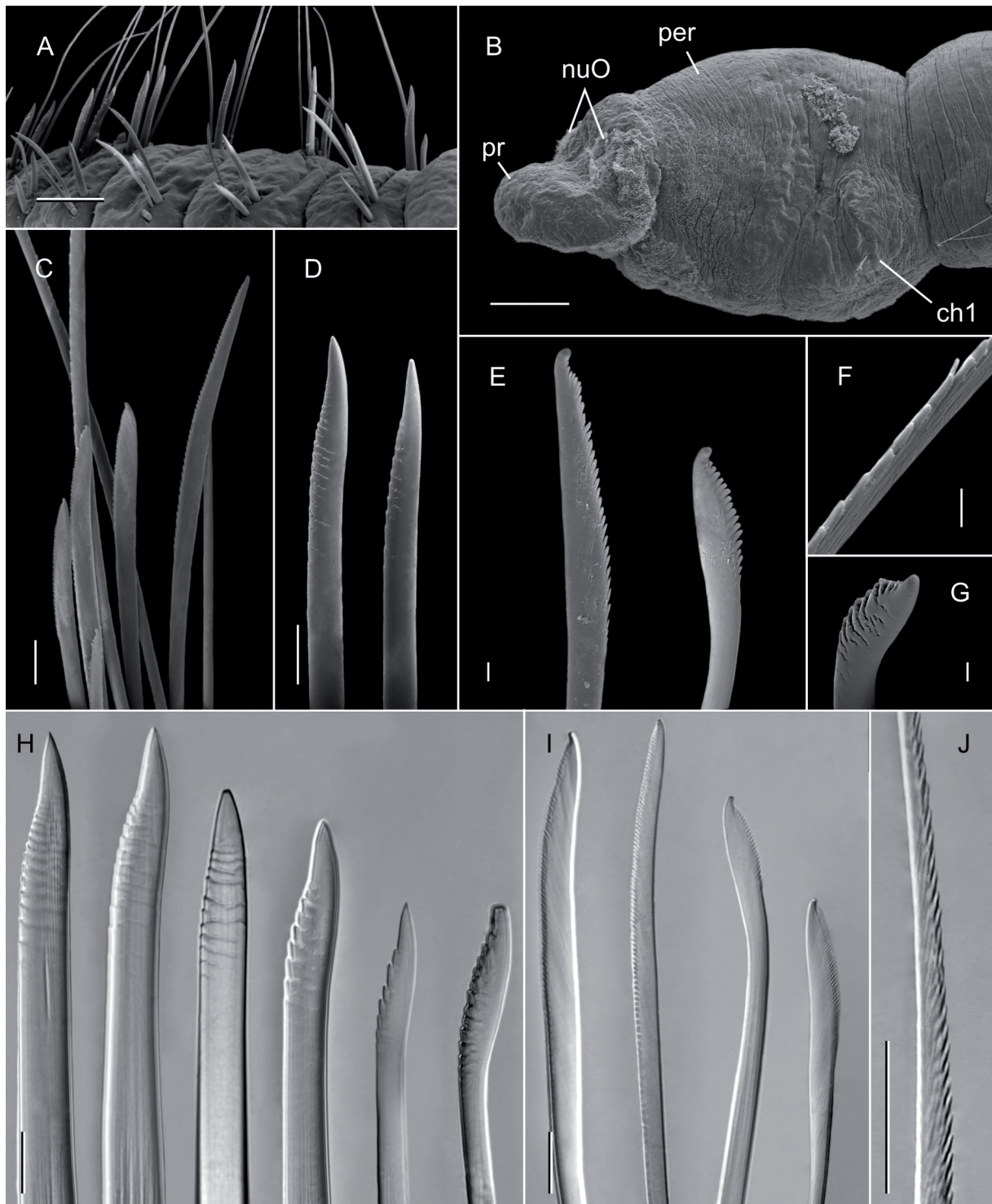
Fig. 9. *Raricirrus arcticus* Buzhinskaja & Smirnov, 2017, details. **A–G**. ZMBN 157684. **H–J**. ZMBN 157685. **A**. Posterior parapodia. **B**. Anterior end, lateral view. **C**. Chaetae of first neuropodium. **D**. Spines. **E**. Pectinate chaetae. **F**. Detail of serrated capillary chaeta. **G**. Detail of spine. **H**. Spines. **I**. Pectinate chaetae. **J**. Detail of serrated capillary chaeta. Abbreviations: ch1 = first chaetiger; nuO = nuchal organ; per = peristomium; pr = prostomium. Scale bars: A–B = 100 μm; C, J = 10 μm; D, G–I = 20 μm; E–F = 2 μm.

Parapodia reduced, chaetae emerging directly from body wall. Anterior and midbody neuropodia with 2–5 capillaries; anterior notopodia with 5–7 capillaries; midbody notopodia with up to 11 chaetae; posterior notopodia with 1–3 chaetae. Capillary chaetae long, in mid-body notopodia few capillaries longer than body width, flat, finely serrated along one edge with distinctly round tip. Neuropodia with 3–5 pectinate chaetae from chaetiger 1–3, finely to coarsely serrated along one edge with distinct rounded tip. Neuropodial pectinate chaetae progressively transitioning to spines, 1–2 per neuropodium; 1–3 per notopodium from posterior third of body; straight along most of their length and curving at tip, pointed, with fine serration on concave side becoming coarser posteriorly (Fig. 9A, C-H).

Pygidium with terminal anus, rounded.

Methylene blue staining pattern

Specimens do not retain any colour except for the tip of the prostomium that stains dark blue.

Comparative remarks

The specimens presented here agree well with the original description, with slight differences in chaetal numbers or distribution and in characters related to the heart body. Differences in chaetal numbers can be attributed to intraspecific variability. In the ethanol fixed specimens available for this study, the heart body was always much darker than described in the original description, and usually only the wide, convoluted part was visible. However, the location of this part of the heart body observed in the material matches well the original description.

Raricirrus arcticus is most similar to *Raricirrus beryli*, the only other species of the genus reported from the area. Differences include morphology, the segment where the heart body starts (segment 2 in *R. arcticus* or 7 in *R. beryli*, Buzhinskaja & Smirnov 2017), and the depth range where they occur: 60–300 m for *R. beryli* (Petersen & George 1991) vs 2000–2500 m for *R. arcticus*. The morphology of nuchal organs has been proposed as a diagnostic character between both species, *R. beryli* was described with nuchal organs without cilia surrounded by ciliary patches and *R. arcticus* was described with nuchal organs inconspicuous among ciliary patches (Buzhinskaja & Smirnov 2017). Nuchal organs in cirratulids have been described as ciliated pits or pits surrounded by cilia and the possibility of eversion of these structures has been proposed as an explanation for the observed variation in this structure (Blake & Magalhães 2017). Personal observations of several species indeed show variation in the shape of nuchal organs due to retraction which could be natural or a consequence of fixation. In particular, specimens of *R. beryli* have been observed with simple rounded ciliary patches on the prostomium without conspicuous non-ciliated nuchal organs (M. Grosse pers. obs.). Therefore, we propose that this character is an artefact and not diagnostic.

Distribution and habitat

Raricirrus arcticus has been recorded from only two locations: the Laptev Sea (Buzhinskaja & Smirnov 2017) and Loki's Castle vent field (Eilertsen *et al*. 2024), from around 2000 to 2500 m deep. At LCVF, it was most common in the Barite Field and the Oasis, but also found on the Eastern Mound at the base of a chimney. *Raricirrus arcticus* is considered to be a chemosynthetic-based ecosystem specialist (Eilertsen *et al*. 2024).

Discussion

Cirratulidae is one of the polychaete families lacking a comprehensive generic revision utilising both molecular and morphological data. Despite low taxon coverage, both *Caulleriella* and *Raricirrus* were recovered as highly supported monophyletic groups corroborating their taxonomic status of valid genera. *Caulleriella jormungandri* sp. nov. can be clearly distinguished from its congeners based on

unambiguous morphological characters. It also shows high levels of genetic divergence from the closely related species in three analysed markers.

The new specimens of *Raricirrus arcticus* from Loki's Castle matched the morphology of the species, considerably expanding its geographical distribution from the Laptev Sea, near the Gakkel ridge, to LCVF on the transition between the Mohns and Knipovich ridges. The distribution of *R. arcticus* resembles that of *Skenea profunda* (Friele, 1879), a gastropod originally described from sunken wood in the Greenland Sea, and later recorded from near the Lomonosov Ridge in the Arctic Ocean (Nekhaev 2022) and from LCVF (Eilertsen *et al.* 2024). Unfortunately, there are no available sequences from the Arctic Ocean for *Raricirrus arcticus* or *Skenea profunda* to compare with the sequences from the Nordic Seas. Obtaining sequence data from specimens collected close to the type locality in species with a wide geographical distribution is always desired but often difficult, especially for the deep-sea species. As of now, we consider the new records from LCVF as belonging to *Raricirrus arcticus* based on morphology. Widely distributed species often represent complexes of either cryptic species or species with minute morphological differences (Hutchings & Kupriyanova 2018; Nygren *et al.* 2018). However, there are some examples of widely distributed species from reducing environments, for example *Sclerolinum contortum* and *Nicomache lokii* which are distributed from the Arctic to the Southern Ocean (Eilertsen *et al.* 2018) or *Raricirrus jennae* which is found both in the East Pacific and in the Southern Ocean (Magalhães *et al.* 2017). This remains to be tested with DNA sequence data for *R. arcticus* by inclusion of additional material into molecular analysis.

Hydrothermal vents host a unique and often habitat-endemic fauna, but the high productivity of vent ecosystems also attracts fauna from background communities, especially in the peripheral areas of the vent field where the environmental conditions are not as challenging (Levin *et al.* 2016). The high abundance of *Caulleriella jormungandri* sp. nov. in the diffuse-venting areas of LCVF, even though this is not a vent-endemic species, indicates an ability to tolerate the reducing conditions of this habitat, allowing them to take advantage of the food-availability. Stable isotope signatures of both *Caulleriella jormungandri* and *Raricirrus arcticus* from LCVF indicate that at least part of their diet is based on chemosynthetic primary production (Eilertsen *et al.* 2024).

Cirratulid polychaetes are often recorded from vents and seeps (e.g., Schander *et al.* 2010; Zapata-Hernández *et al.* 2014; Alalykina 2022). However, they are generally only identified to family or genus level at best. More comprehensive and focused efforts on this understudied group at different vent sites might reveal additional diversity and contribute to a better understanding of hydrothermal vents ecosystems.

Deep-sea ecosystems face numerous anthropogenic threats, with deep-sea mining being a particularly concerning factor (Danovaro *et al.* 2020). Given these risks, it becomes increasingly essential to deepen our knowledge of biodiversity at hydrothermal vents and identify and describe new species. Such efforts are crucial in understanding how these ecosystems may respond to disturbances in the face of impending threats (Van Dover *et al.* 2018), and to enable conservation efforts and environmental monitoring.

Hydrothermal vent fauna is geographically segregated, with around 95% of species restricted to one biogeographic region (Moalic *et al.* 2012). The vent fauna of the Arctic Mid-Ocean Ridges is generally very distinct from what is known from vents on the Mid-Atlantic Ridge (Eilertsen *et al.* 2024). However, two species have been found to have a broader distribution. *Nicomache lokii* has been found in the Arctic Ocean, the Antarctic Ocean and Barbados Trench while *Sclerolinum contortum* has been found in the Arctic Ocean, the Antarctic Ocean and the Gulf of Mexico (Eilertsen *et al.* 2018). The Arctic (including the Nordic Seas) has been proposed as a separate biogeographic province for bathyal fauna, (Maureaud *et al.* 2023), but global biogeographic analyses of hydrothermal vent fauna have thus far not included Arctic vents (e.g., Moalic *et al.* 2012; Rogers *et al.* 2012). The distribution of *R. arcticus*,

as revealed in this study, further supports the idea of potential connectivity between the Nordic Seas and the Arctic Ocean (Oug *et al*. 2017). To ensure effective conservation and management, it becomes imperative to comprehend the intricacies of biodiversity and genetic connectivity among different vent sites (Vrijenhoek 2010; Eilertsen *et al*. 2024). By doing so, we can better safeguard these unique and vulnerable deep-sea ecosystems.

Acknowledgements

References

Alalykina I.L. 2022. Composition and distribution of polychaete assemblages associated with hydrothermal vents and cold seeps in the Bering Sea. *Deep Sea Research Part II: Topical Studies in Oceanography* 206: 105192. https://doi.org/10.1016/j.dsr2.2022.105192

Blake J. 2018. Bitentaculate Cirratulidae (Annelida, Polychaeta) collected chiefly during cruises of the R/V *Anton Bruun*, USNS *Eltanin*, USGC *Glacier*, R/V *Hero*, RVIB *Nathaniel B. Palmer*, and R/V *Polarstern* from the Southern Ocean, Antarctica and off Western South America. *Zootaxa* 4537 (1): 1–130. https://doi.org/10.11646/zootaxa.4537.1.1

Blake J.A. 2019. New species of Cirratulidae (Annelida, Polychaeta) from abyssal depths of the Clarion-Clipperton Fracture Zone, North Equatorial Pacific Ocean. *Zootaxa* 46292 (2): 151–187. https://doi.org/10.11646/zootaxa.4629.2.1

Blake J. 2021. New species and records of *Caulleriella* (Annelida, Cirratulidae from shelf and slope depths of the Western North Atlantic Ocean. *Zootaxa* 4990 (2): 253–279. https://doi.org/10.11646/zootaxa.4990.2.3

Blake J. & Magalhães W.F. 2017. Family Cirratulidae Ryckholt, 1851. *In*: Westheide W. & Purschke G. (eds) *Handbook of Zoology, a Natural History of the Phyla of the Animal Kingdom*. Walter de Gruyter GmbH & Co. KG, Berlin/Boston.

Brix S., Meissner K., Stransky B., Halanych K., Jennings R.M. & Svavarsson J. 2014. The IceAGE project — a follow up of BIOICE. *Polish Polar Research* 35 (2): 141–150.

Buzhinskaja G.N. & Smirnov R.V. 2017. A new species of *Raricirrus* (Polychaeta, Ctenodrilidae) from the continental slope of the the Laptev Sea near the Gakkel Ridge. *Proceedings of the Zoological Institute of the Russian Academy of Science* 321(4): 425–432. https://doi.org/10.31610/trudyzin/2017.321.4.425

Carr C.M., Hardy S.M., Brown T.M., Macdonald T.A. & Hebert P.D.N. 2011. A Tri Oceanic Perspective: DNA Barcoding reveals geographic structure and cryptic diversity in Canadian polychaetes. *PLoS ONE* 6: e22232. https://doi.org/10.1371/journal.pone.0022232

Chamberlin R.V. 1919. The Annelida Polychaeta [Albatross Expeditions]. *Memoirs of the Museum of Comparative Zoology at Harvard College* 48: 1–514. https://doi.org/10.5962/bhl.title.49195

Danovaro R., Fanelli E., Aguzzi J., Billet D., Carugati L., Corinaldesi C., Dell'Anno A., Gjerde K., Jamieson A.J., Kark S., McClain C., Levin L., Levin N., Ramirez-Llodra E., Ruhl H., Smith C.R., Snelgrove P.V.R., Thomsen L., Van Dover C.L. & Yasuhara M. 2020. Ecological variables for developing a global deep-ocean monitoring and conservation strategy. *Nature Ecology and Evolution* 4: 181–192. https://doi.org/10.1038/s41559-019-1091-z

Dean H.K. 1995 A new species of *Raricirrus* (Polychaeta: Ctenodrilidae) from wood collected in the Tongue of the Ocean, Virgin Islands. *Proceedings of the Biological Society of Washington* 108 (2): 169–179.

Dean H.K. & Blake J.A. 2007. *Chaetozone* and *Caulleriella* (Polychaeta: Cirratulidae) from the Pacific Coast of Costa Rica, with the description of eight new species. *Zootaxa* 1451: 41–68. https://doi.org/10.11646/zootaxa.1451.1.2

Edgard R.C. 2004. MUSCLE: multiple sequence alignment with high accuracy and high throughput. *Nucleic acids research* 32 (5): 1792–1799. https://doi.org/10.1093/nar/gkh340

Eilertsen M.H., Georgieva M.N., Kongsrud J.A., Linse K., Wiklund H., Glover A.G. & Rapp H.T. 2018. Genetic connectivity from the Arctic to the Antarctic: *Sclerolinum contortum* and *Nicomache lokii* (Annelida) are both widespread in reducing environments. *Scientific Reports* 8: 4810. https://doi.org/10.1038/s41598-018-23076-0

Eilertsen M.H., Kongsrud J.A., Tandberg A.H.S., Alvestad T., Budaeva N., Martell L., Ramalho S.P., Falkenhaug T., Huys R., Oug E., Bakken T., Høisæter T., Rauch C., Carvalho F.C., Savchenko A.S., Ulvatn T., Kongshavn K., Berntsen C.M., Rydland Olsen B. & Pedersen R.B. 2024. Diversity, habitat endemicity and trophic ecology of the fauna of Loki's Castle vent field on the Arctic Mid-Ocean Ridge. *Scientific Reports* 14: 103. https://doi.org/10.1038/s41598-023-46434-z

Folmer O., Black M., Hoeh W., Lutz R. & Vrijenhoek R. 1994. DNA primers for amplification of mitochondrial cytochrome c oxidase subunit I from diverse metazoan invertebrates. *Molecular Marine Biology and Biotechnology* 3: 294–299.

Geller J., Meyer C., Parker M. & Hawk H. 2013. Redesign of PCR primers for mitochondrial cytochrome c oxidase subunit I for marine invertebrates and application in all-taxa biotic surveys. *Molecular Ecology Resources* 13: 851–861. https://doi.org/10.1111/1755-0998.12138

Hartman O. 1961. Polychaetous annelids from California. *Allan Hancock Pacific Expeditions* 25: 1–226. Available from https://www.biodiversitylibrary.org/page/5214802 [accessed 15 Nov. 2024].

Hoang D.T., Chernomor O., von Haeseler A., Minh B.Q. & Vinh L.S. 2018. UFBoot2: Improving the Ultrafast Bootstrap approximation. *Molecular Biology and Evolution* 35 (2): 518–522. https://doi.org/10.1093/molbev/msx281

Hutchings P. & Kupriyanova E. 2018. Cosmopolitan polychaetes – fact or fiction? Personal and historical perspectives. *Invertebrate Systematics* 32 (1): 1–9. https://doi.org/10.1071/IS17035

Jimi N., Fujimoto S., Fujiwara Y., Oguchi K. & Miura T. 2022. Four new species of *Ctenodrilus*, *Raphidrilus*, and *Raricirrus* (Cirratuliformia, Annelida) in Japanese waters, with notes on their phylogenetic position. *PeerJ* 10: e13044. https://doi.org/10.7717/peerj.13044

Kalyaanamoorthy S., Minh B.Q., Wong T.K.F., von Haeseler A. & Jermiin L.S. 2017. ModelFinder: Fast model selection for accurate phylogenetic estimates. *Nature Methods* 14: 587–589. https://doi.org/10.1038/nmeth.4285

Katoh K., Rozewicki J. & Yamada K.D. 2017. MAFFT online service: multiple sequence alignment, interactive sequence choice and visualization. *Briefings in Bioinformatics* 20 (4): 1160–1166. https://doi.org/10.1093/bib/bbx108

Kelley D.S. & Shank T.M. 2010. Hydrothermal systems: A decade of discovery in slow spreading environments. *In*: Rona P.A., Devey C.W., Dyment J. & Murton B.J. (eds) *Diversity of Hydrothermal Systems on Slow Spreading Ocean Ridges*.

Kongsrud J.A. & Rapp H.T. 2012. *Nicomache* (*Loxochona*) *lokii* sp. nov. (Annelida: Polychaeta: Maldanidae) from the Loki's Castle vent field: an important structure builder in an Arctic vent system. *Polar Biology* 35: 161–170. https://doi.org/10.1007/s00300-011-1048-4

Kongsrud J.A., Eilertsen M.H., Alvestad T., Kongshavn K. & Rapp H.T. 2017. New species of Ampharetidae (Annelida: Polychaeta) from the Arctic Loki Castle vent field. *Deep Sea Research Part II: Topical Studies in Oceanography* 137: 232–245. https://doi.org/10.1016/j.dsr2.2016.08.015

Langerhans P. 1880. Die Wurmfauna von Madeira. III. *Zeitschrift für wissenschaftliche Zoologie* 34 (1): 87–143. Available from https://www.biodiversitylibrary.org/page/42353743 [accessed 15 Nov. 2024].

Larsson A. 2014. AliView: A fast and lightweight alignment viewer and editor for large datasets. *Bioinformatics* 30 (22): 3276–3278. https://doi.org/10.1093/bioinformatics/btu531

Le H.L.V., Lecointre G. & Perasso R. 1993. A 28S rRNA based phylogeny of the gnathostomes: First steps in the analysis of conflict and congruences with morphologically based cladograms. *Molecular Phylogenetics and Evolution* 2 (1): 31–51. https://doi.org/10.1006/mpev.1993.1005

Letunic I. & Bork P. 2021. Interactive Tree Of Life (iTOL) v5: An online tool for phylogenetic tree display and annotation. *Nucleic Acids Research* 49 (1): 293–296. https://doi.org/10.1093/nar/gkab301

Levin L.A., Baco A.R., Bowden D.A., Colaco A., Cordes E.E., Cunha M.R., Demopoulos A.W.J., Gobin J., Grupe B.M., Le J., Metaxas A., Netburn A.N., Rouse G.W., Thurber A.R., Tunnicliffe V., Van Dover C.L., Vanreusel A. & Watling L. 2016. Hydrothermal vents and methane seeps: Rethinking the sphere of influence. *Frontiers in Marine Science* 3: 72. https://doi.org/10.3389/fmars.2016.00072

Magalhães W.F., Linse K. & Wiklund H. 2017. A new species of *Raricirrus* (Annelida: Cirratuliformia) from deep-water sunken wood off California. *Zootaxa* 4353 (1): 51–68. https://doi.org/10.11646/zootaxa.4353.1.3

Maureaud A.A., Reygondeau G., Ingenloff K., Vigneron J.C., Watling L., Winner K. & Jetz W. 2023. A global biogeographic regionalization of the benthic ocean. Preprint. https://doi.org/10.31219/osf.io/nkjvf

Meca M.A., Kongsrud J.A., Kongshavn K., Alvestad T., Meißner K. & Budaeva N. 2024. Diversity of *Orbiniella* (Orbiniidae, Annelida) in the North Atlantic and the Arctic. *ZooKeys* 1205: 51–88. https://doi.org/10.3897/zookeys.1205.120300

McIntosh W.C. 1916. Notes from the Gatty Marine Laboratory, St. Andrews. No. 39.1. On the colouration of *Caesicirrus neglectus*, Arwidsson. 2. On *Cirratulus* (*bioculatus*) *incertus*, M'I. 3. On the British Serpulidae, with a note of those procured in the 'Porcupine' Expeditions and those obtained by Canon Norman in Norwegian waters. 4. On a *Placostegus*, from the 'Porcupine' Expedition of 1870. *Annals and Magazine of Natural History, Series 8* 18: 161–199. https://doi.org/10.1080/00222931608693835

Miller M.A., Pfeiffer W. & Schwartz T. 2010. Creating the CIPRES Science Gateway for inference of large phylogenetic trees. *Proceedings of the Gateway Computing Environments Workshop (GCE), 14 Nov. 2010, New Orleans, LA*: 1–8. https://doi.org/10.1109/GCE.2010.5676129

Minh B.Q., Schmidt H.K., Chernomor O., Schrempf D., Woodhams M.D., von Haeseler A. & Lanfear R. 2020. IQ-TREE 2: New models and efficient methods for phylogenetic inference in the genomic era. *Molecular Biology and Evolution* 37 (5): 1530–1534. https://doi.org/10.1093/molbev/msaa015

Moalic Y., Desbruyères D., Duarte C.M., Rozenfeld A.F., Bachraty C. & Arnaud-Haond S. 2012. Biogeography revisited with network theory: retracing the history of hydrothermal vent communities. *Systematic Biology* 61 (1): 127. https://doi.org/10.1093/sysbio/syr088

Nekhaev I. 2022. *Skenea profunda* (Vetigastropoda: Skeneidae) in the central Arctic. *Ruthenica* 32 (2): 105–109. https://doi.org/10.35885/ruthenica.2022.32(3).2

Nygren A., Parapar J., Pons J., Meißner K., Bakken T., Kongsrud J.A., Oug E., Gaeva D., Sikorski A., Johansen R.A., Hutchings P.A., Lavesque N. & Capa M. 2018. A mega-cryptic species complex hidden among one of the most common annelids in the North East Atlantic. *PLoS ONE* 13 (6): e0198356. https://doi.org/10.1371/journal.pone.0198356

Oug E., Bakken T., Kongsrud J.A. & Alvestad T. 2017. Polychaetous annelids in the deep Nordic Seas: Strong bathymetric gradients, low diversity and underdeveloped taxonomy. *Deep Sea Research Part II: Topical Studies in Oceanography* 137: 102–112. https://doi.org/10.1016/j.dsr2.2016.06.016

Palumbi S.R. 1996. Nucleic acid II: The polymerase chain reaction. *In*: Hillis D.M. & Mable B.K. (eds) *Molecular Systematics*: 205–247. Sinauer Associates, Sunderland, MA.

Passamaneck Y.J., Schander C. & Halanych K.M. 2004. Investigation of molluscan phylogeny using large-subunit and small-subunit nuclear rRNA sequences. *Molecular Phylogenetics and Evolution* 32 (1): 25–38. https://doi.org/10.1016/j.ympev.2003.12.016

Pedersen R.B., Rapp H.T., Thorseth I.H., Lilley M.D., Barriga F.J., Baumberger T., Flesland K., Fonseca R., Früh-Green G.L. & Jorgensen S.L. 2010. Discovery of a black smoker vent field and vent fauna at the Arctic Mid-Ocean Ridge. *Nature Communications* 1: e126. https://doi.org/10.1038/ncomms1124

Portail M, Olu K., Dubois S.F., Escobar-Briones E., Gelinas Y., Menot L. & Sarrazin J. 2016. Food-web complexity in Guaymas Basin hydrothermal vents and cold seeps. *PLoS ONE* 11 (9): e0162263. https://doi.org/10.1371/journal.pone.0162263

Ramirez-Llodra E., Shank T.M. & German C.R. 2007. Biodiversity and biogeography of hydrothermal vent species: thirty years of discovery and investigations. *Oceanography* 20: 30–41. https://doi.org/10.5670/oceanog.2007.78

Ritt B., Sarrazin J., Caprais J.-C., Noël P., Gauthier O., Pierre C., Henry P. & Desbruyères D. 2010. First insights into the structure and environmental setting of cold-seep communities in the Marmara Sea. *Deep Sea Research Part I: Oceanographic Research Papers* 57 (9): 1120–1136. https://doi.org/10.1016/j.dsr.2010.05.011

Rogers A.D., Tyler P.A., Connelly D.P., Copley J.T., James R., Larter R.D., Linse K., Mills R.A., Naveira Garabato A., Pancost R.D., Pearce D.A., Polunin N.V.C., German C.R., Shank T., Boersch-Supan P.H., Alker B.J., Aquilina A., Bennett S.A., Clarke A., ... & Zwirglmaier K. 2012. The discovery of new deep-sea hydrothermal vent communities in the Southern Ocean and implications for biogeography. *PLoS Biology* 10 (1): e1001234. https://doi.org/10.1371/journal.pbio.1001234

Schander C., Rapp H.T., Kongsrud J.A., Bakken T., Berge J., Cochrane S., Oug E., Byrkjedal I., Todt C., Cedhagen T., Fosshagen A., Gebruk A., Larsen K., Levin L., Obst M., Pleijel F., Stöhr S., Warén A.,

Mikkelsen N.T., ... & Pedersen R.B. 2010. The fauna of hydrothermal vents on the Mohn Ridge (North Atlantic). *Marine Biology Research* 6 (2): 155–171. https://doi.org/10.1080/17451000903147450

Sellanes J., Zapata-Hernández G., Pantoja S. & Jessen G.L. 2011. Chemosynthetic trophic support for the benthic community at an intertidal cold seep site at Mocha Island off central Chile. *Estuarine, Coastal and Shelf Science* 95 (4): 431–439. https://doi.org/10.1016/j.ecss.2011.10.016

Struck T.H., Purschke G. & Halanych K.M. 2006. Phylogeny of Eunicida (Annelida) and exploring data congruence using a Partition Addition Bootstrap Alteration (PABA) approach. *Systematic Biology* 55 (1): 1–20. https://doi.org/10.1080/10635150500354910

Sweetman A.K., Levin L.A., Rapp H.T. & Schander C. 2013. Faunal trophic structure at hydrothermal vents on the southern Mohn's Ridge, Arctic Ocean. *Marine Ecology Progress Series* 473: 115–131. https://doi.org/10.3354/meps10050

Van Dover C.L. German C.R., Speer, K.G., Parson L.M. & Vrijenhoek R.C. 2002. Evolution and biogeography of deep-sea vent and seep invertebrates. *Science* 295: 1253–1257. https://doi.org/10.1126/science.1067361

Van Dover C.L., Anraud-Haond S., Gianni M., Helmreich S., Huber J.A., Jaeckel A., Metaxas A., Pendleton L.H., Petersen S. & Ramirez-Llodra E. 2018. Scientific rationale and international obligations for protection of active hydrothermal vent ecosystems from deep-sea mining. *Marine Policy* 90: 20–28. https://doi.org/10.1016/j.marpol.2018.01.020

Vrijenhoek R.C. 2010. Genetic diversity and connectivity of deep-sea hydrothermal vent metapopulations. *Molecular Ecology* 19 (20): 4391–4411. https://doi.org/10.1111/j.1365-294X.2010.04789.x

Zapata-Hernández G., Sellanes J., Thurber A.R., Levin L.A., Chazalon F. & Linke P. 2014. New insights on the trophic ecology of bathyal communities from the methane seep area off Concepción, Chile (~36° S). *Marine Ecology* 35 (1): 1–21. https://doi.org/10.1111/maec.12051

Supplementary files

Supp. file 1. List of material examined and specimens used in molecular analyses with collection data, BOLD ID and GenBank accession numbers. https://doi.org/10.5852/ejt.2025.987.2855.12969

Supp. file 2. DNA alignments. https://doi.org/10.5852/ejt.2025.987.2855.12971

Supp. file 3. Distance matrices. https://doi.org/10.5852/ejt.2025.987.2855.12973

Supp. file 4. Phylogenetic trees. https://doi.org/10.5852/ejt.2025.987.2855.12975

Supp. file 5. PCR primers and protocols. https://doi.org/10.5852/ejt.2025.987.2855.12977